A prototype system for earthquake early-warning and alert management in southern Italy

Iannaccone G.[1*], Zollo A.[2], Elia L.[3], Convertito V.[1], Satriano C.[3], Martino C. [3], Festa G. [2], Lancieri M. [1], Bobbio A. [1], Stabile T.A. [3], Vassallo M. [3], Emolo A. [2]

(1) Istituto Nazionale di Geofisica e Vulcanologia, Osservatorio Vesuviano, via Diocleziano 328, 80124 Naples, Italy
(2) Università di Napoli "Federico II", Dipartimento di Scienze Fisiche, Complesso Universitario Monte Sant'Angelo, via Cinthia, Naples, Italy
(3) AMRA scarl, via Nuova Agnano 11, 80125 Naples, Italy

Keywords: accelerometric network; earthquake early warning; real-time data analysis; southern Apennines

[*] Corresponding author: Giovanni Iannaccone, iannaccone@ov.ingv.it

Abstract

The Irpinia Seismic Network (ISNet) is deployed in Southern Apennines along the active fault system responsible for the 1980, November 23, M_S6.9 Campania-Lucania earthquake. It is set up by 27 stations and covers an area of about 100x70 km^2. Each site is equipped with a 1-g full-scale accelerometer and a short-period velocimeter. Due to its design characteristics, i.e. the wide dynamic range and the high density of stations, the ISNet network is mainly devoted to estimating in real-time the earthquake location and magnitude from low- to high- magnitude events, and to providing ground-motion parameters values so to get some insights about the ground shaking expected. Moreover, the availability of high-quality of data allows studying the source processes related to the seismogenetic structures in the area. The network layout, the data communication system and protocols and the main instrumental features are described in the paper. The data analysis is managed by Earthworm software package that also provides the earthquake location while homemade software has been developed for real-time computation of the source parameters and shaking maps. Technical details about these procedures are given in the article. The data collected at the ISNet stations are available upon request.

Introduction

Over the last few centuries, the southern Apennines have been struck by several strong earthquakes, the last of which occurred on 23 November, 1980 (Ms=6.9). This resulted in more than 3,000 casualties and extensive damage throughout the area. In terms of the scientific literature, this last earthquake has been one of the most studied of those that have occurred in the Mediterranean area (Westaway and Jackson, 1984; Bernard and Zollo, 1989). Similarly, many studies have investigated the crustal structure underneath the Apennine chain, to provide constraints for the geodynamic evolution in this sector of the Mediterranean region, and specifically to obtain seismic-wave propagation models, which are the

key elements for all seismological studies (Chiarabba and Amato, 1996; Improta et al, 2000; 2003).

At present, the southern Apennines, and in particular the Irpinia area, are characterized by a background of continuous seismic activity that is probably connected to the seismogenetic fault system that generated the 1980 main shock. Magnitudes here are generally lower than 3, with occasional greater magnitude events, like the earthquake on 3 April, 1996 (M_L = 4.9). At the southern border of the Irpinia seismogenetic fault system, these moderate energy events occur mainly with strike-slip mechanisms, with a preferred fault plane oriented in the E-W direction (i.e. the 1990-1991 seismic sequences, with M 5.2 and M 4.4, respectively).

Finally, based on an analysis of historic and recent seismicity, and according to a seismotectonic regionalization of the Italian peninsula, Boschi et al. (1995) have indicated a probability in the range 0.22-0.41 for the occurrence of an earthquake of M ≥5.9 in the Irpinia region in the next 20 years. Similarly, Cinti et al. (2004) have provided a probability map of M >5.5 earthquakes predicted over the next 10 years in Italy, and they indicate that the Campania-Lucania sector of the southern Apennines has one of the highest probabilities of occurrence.

In 2005, with the financial support of the local government of Regione Campania, the development of the local seismic network in the southern Apennines started. This is known as ISNet, the Irpinia Seismic Network, and it is designed around two main concepts: (i) to provide high quality data for studies relating to seismogenic faults in the area; and (ii) to test a prototype system for earthquake early warning and post-event warning for the protection of strategically relevant infrastructure in the Campania region.

ISNet was set-up to acquire strong-motion records of large earthquakes near to their source, along with very low magnitude local events, and records of distant earthquakes (teleseisms). Consequently, each seismic station is equipped with an accelerometer with a 1-g dynamic range and short-period seismometers; furthermore, selected sites are equipped with broad-band sensors.

To realize an earthquake early-warning system that is reliable and as robust as possible, we considered several constraints in the planning stage of the hardware of the network. Examples here include redundancy in the telecommunication pathways, so as to avoid data loss in the case of failure of a

radio link, and the storing and analysis of data, which are performed on different sites distributed throughout the area of the network. This has been realized by organizing the network into 'sub-nets', each of which is managed by a data concentrator (LCC, Local Control Center). Each node of the network can process and analyze the seismic waveforms acquired in real-time, and can provide the measured quantities to its closest LCC. As more stations record a seismic signal, the new measurements are sent to and processed by the LCCs, which cross-check the information coming from the different stations. This provides an output of progressively refined estimations of the earthquake location and magnitude, along with the associated uncertainties.

Similarly, to ensure the reliability of the final results, we have combined different methodologies for the performing of the main analysis for early-warning purposes, and we have developed software for real-time monitoring of the functional status of the main components of this seismic network. This monitoring will allow the early-warning system to be closely managed, to maintain its functionality. The software is thus now in use by the staff of ISNet, to manage, monitor and maintain the instrumentation, and by researchers, to access, analyze and edit the seismic data that is being acquired. It also constitutes the means through which the seismogram recordings and the data produced are made available to scientific users.

This paper describes the characteristics of this earthquake early-warning system that has been developed and is now under testing in southern Italy, providing the technical aspects of its core infrastructure, the ISNet, and describing its functional modalities.

ISNet layout and instruments

ISNet is a high dynamic range, dense seismographic network, that has been deployed in southern Italy, along the Campania-Lucania Apennines (Weber et al., 2007). The network covers an area of about 100 km × 70 km, over the active seismic faults system that generated the 1980, M=6.9, Irpinia earthquake (Figure 1). It constitutes the core infrastructure for a regional Earthquake Early-Warning System (EEWS) that remains under development today. ISNet is primarily aimed at providing an alert to selected target sites in the Campania Region upon the

occurrence of moderate to large earthquakes (M>4), and to promptly compute regional ground-shaking maps.

ISNet is currently composed of 27 seismic stations and five LCC data storage and processing sites. All of the stations are equipped with a strong-motion accelerometer (Güralp CMG-5T) and a three-component velocity meter (Geotech S-13J), with a natural period of one second, thus ensuring a high dynamic recording range. Five stations feature a broad-band velocity meter (Nanometrics Trillium, 0.025-50 Hz), to record regional and teleseismic events and to provide useful data for analysis of ambient seismic noise, which is aimed at obtaining a shear-velocity model of the region. The full recording dynamic range is $\pm 1g$, and the sensitivity is sufficient to record M 1.5 events at a distance of more than 40 km.

The seismic stations are housed in shelters, each of which is equipped with two solar panels and two batteries. The data acquisition from the six channels is performed by a Linux based embedded computer (74 MHz ARM CPU), connected to a GPS receiver, and with a removable Compact Flash card (5 GB) for local data archiving. The data logger from each station communicates with its closest LCC through the Wi-Fi directional antennae and a wireless bridge. Sensor data is thus continuously transmitted to remote servers too, for further archiving and processing. Each station also houses a programmable device that is equipped with a GSM modem, to send environmental data from the shelter (battery levels, open door, fire alarm) in the form of text messages, either automatically or on demand.

The stations are positioned within two imaginary concentric ellipses, about 10 km apart, with their major axes parallel to the Apennine chain. In the outer ellipse, the average distance between stations is 20 km, in the inner ellipse it is 10 km. The network topology features multiple star-shaped sub-networks, with a few stations and an LCC at their center. This ensures a fast and robust distributed data analysis, through the multiple processing nodes, and a redundant and fully digital communication infrastructure: a wireless radio link between each seismic station and its nearest LCC; a higher bandwidth wireless backbone (under deployment) between LCCs; redundant connections between the LCCs and the network control center (NCC), located in Naples (Figure 1).

Finally, before installation, the sensor/ data-logger pairs were fully calibrated for single-channel responses by an automated process. This calibration covers the entire frequency spectrum, and uses the LabVIEW/MatLab software package that provides the transfer function in graphical mode and in terms of poles and zero.

Real-time data management

The real-time data management and analysis of ISNet is realized through several levels that match the physical structure of the network (Figure 2). The first level is the data logger, where the signal is digitized and time-stamped. From each single physical channel, the data logger can provide several virtual channels, with different sampling rates.

Each data logger uses the SeedLink protocol (http://www.iris.edu/data/dmc-seedlink.htm) to send a real-time waveform data stream to the associated LCC. This runs the SeisComP software (Hanka et al., 2001), which acts as a hub for data collection and distribution. Indeed, external users can obtain real-time data streams from ISNet stations by connecting to one or more LCCs, using the SeedLink protocol. On top of SeisComP, each LCC runs the Earthworm real-time analysis software (Johnson et al., 1995), which processes data streams and performs filtering and automatic P-phase picking. The permanent storage for data streams managed by Earthworm is performed at each LCC using the Winston Wave Server software package (http://www.avo.alaska.edu/Software/winston/W_Manual_TOC.html). This software keeps a MySQL database of continuous waveforms and provides segments of data on request. Moreover, Winston can serve a request for several days worth of data as an image (helicorder), and for the day-to-day monitoring of the stations. Since just an image is sent from the LCC to the requesting client, and not the actual data, this feature helps save bandwidth.

An Earthworm installation running at the NCC performs the event detection. This centralizes all of the phase readings coming from the LCCs and performs phase association and event location using the “binder” module. The

binder computes the time difference between every pair of P arrivals and performs a back-projection of this value, to search for a volume within a spatial grid where the hypocenter is likely to be. When six or more consistent arrival times are detected, a new event is declared. After its declaration each event is relocated by an L1-norm, linearized algorithm, which uses the previously determined hypocenter as its starting point. If new arrivals enter the binder, these are first checked against the active events, or, should it be the case, used to declare a new event.

The waveform and parametric data (source location and origin time) for each event detected are stored in a database, the details of which are provided in the next sections. The automatic event detection is at the basis of our near real-time analysis system, which will be discussed hereinafter.

The ISNet near real-time analysis system

The Earthworm seismic management software that runs at each LCC and at the NCC is capable of real-time analysis. It provides a number of modules to perform common tasks, like estimating the local magnitude or measuring the peak ground values for ground shaking-map computation. However, implementing a new feature as an Earthworm module is not a trivial task, since it requires a good knowledge of the C programming language and a careful handling of the input/output routines.

For this reason we decided to make use of Earthworm up to the automatic event detection (performed at the NCC by the "binder_ew" module), while we designed a custom, near real-time, system for computation of earthquake source parameters and ground-shaking maps. The basic idea behind this system is that a seismologist who is able to write the computer code to analyze off-line data could easily make his work part of a near real-time processing chain, regardless of the programming language he uses and without entering into the details of the input/output strategies. We based our system on three key concepts: simplicity, flexibility and extendibility.

An outline of the ISNet near real-time analysis system is shown in Figure 3. The system is structured as a processing chain, where each module is executed once the previous one terminates. The chain is launched every 2 min: the next

instance of the chain can process a new event while the previous event is still processed by the earlier instance. The modules can be logically divided in two families:

- *Core modules*. These are designed to interact with Earthworm, to: build a list of events (00_parse_events); keep track of the P-arrival times used for event association (01_parse_picks); and download event waveforms from the Earthworm wave server and save them as sac files (02_get_traces and 06_get_full_traces). Core modules are connected to the underlying network management system and need to be replaced by equivalent modules if a different system is used.

- *User defined modules*. These modules only rely on the existence of an event file (with event id, and location, as reported by the binder), a pick file, and the waveforms (in sac format) associated to each event.

All of the modules are written as Linux Bash shells, although this is not mandatory. Several modules make use internally of sac macros, awk scripts and/or custom Fortran code.

The results of the automatic analyses are published on an interactive web page, called “ISNet Bulletin” (Figure 4). This page is designed around a Google map, which covers the upper half of the page, and shows the event locations and the stations. The default view is centered on ISNet, but it is possible to zoom in and out. The second half of the page shows a table view of the events, with the associated parameters. The fields are: event id, origin date, origin time, latitude, longitude, depth, ML, MW, place (toponym), number of triggered stations, S-displacement spectra, and ground-shaking maps. The methodologies used to compute all of these parameters are explained in the following paragraphs.

Some of these entries are clickable, and provide additional information. For instance, clicking on the number of triggered stations pops up a window with the recorded waveforms, while for a click on the place name, a balloon appears on the map with detailed information of the event. This includes origin time, ML, location, and focal mechanism if available. Finally, the controls in the last column allow you to display the ground-shaking map on a Google map, for peak ground

acceleration (PGA), peak ground velocity (PGV) and instrumental intensity, or a plot of the measured peak ground values.

Real-time analysis for early-warning purposes

For the real-time analysis for early-warning applications we are developing a stand-alone software system, SeismNet Alarm, that is currently deployed at the Network Control Center in Naples for testing the performance analysis. SeismNet Alarm is implemented by a C++ application, and it can process the live stream of the three-component acceleration recorded at all of the stations. Alternatively, it can run in simulation mode, whereby it uses locally stored files that contain the waveforms recorded by the stations for relevant events that have happened in the past. In real-time mode, the application needs to retrieve the station data in SeedLink format. Hence, for each station, it creates a processing thread that opens a connection with the SeedLink server running at the relevant LCC, implemented by SeisComP. Each thread is in charge of retrieving and buffering the data, and carrying out the automatic P-wave-arrival detection. The main processing thread takes care of binding picks from several stations to an event identifier, thus detecting an event, locating the hypocenter and determining the event magnitude. The main steps performed by this system are thus the following:

- **Arrival detection**. We currently run a picking algorithm, based on that of Baer and Kradolfer on each vertical component. This produces an arrival time and its associated uncertainty for each station.
- **Picks binding**. This phase determines whether new picks from the stations are compatible with a new event that has just occurred, or with an ongoing event already declared, rather than due to unrelated local phenomena, such as anthropogenic or environmental noise. Several sets of information are exploited to perform this step, such as the temporal coincidence of the picks at several stations, the time sequence of the picks and the location of the triggering sites.
- **Event location**. This step is performed by the RTLoc algorithm (Satriano et al., 2008), an evolutionary, real-time location technique based on an equal

differential time (EDT) formulation and a probabilistic approach for describing the hypocenter. The location estimate is not only based on the arrival times at the stations that are triggered, but also takes into account that at the time of each computation some stations may not have been triggered. With just one recorded arrival, the hypocentral location is constrained by the Voronoi cell around the first triggering station, which is constructed using the travel times to the not-yet-triggered stations. With two or more triggered arrivals, the location is constrained by the intersection of the volume defined by the Voronoi cells for the remaining, not-yet-triggered stations, and the EDT surfaces between all pairs of triggered arrivals. As time passes, and more triggers become available, the evolutionary location converges to a standard EDT location.

- **Event magnitude estimation**. The recorded acceleration is band-pass filtered to focus on low frequencies, and converted to the overall peak displacement of the ground. This is done over two temporal windows, starting at the measured P-wave arrival and the estimated S-wave arrival, encompassing 2 s to 4 s of signal. An empirical relationship that correlates the final event magnitude with the logarithm of these quantities and the distance from the event to the station is then used to yield a magnitude for each station. These are in turn combined to produce an early estimate of the event magnitude, and of its uncertainty, which evolves while the earthquake is occurring.

Each of the steps from event detection onwards triggers an alarm message that can be sent over a dedicated network line to selected target sites. While the event propagates at a speed of around 3.5 km/s from the its origin to the target, the alarm messages can be sent almost instantly to front-end applications running at the target site that can, for instance, initiate an automatic shut down procedure of an infrastructure. For a destructive earthquake occurring in the Irpinia region, and a target site in the city of Naples, this means that there is an interval of the order of 20 s from when the alarm reaches the target, to when the destructive waves arrive there.

For resilience to failures of the early-warning system or the network, which will be somewhat more likely while an energetic event is occurring, a future goal is to deploy several instances of the system within the network, at each

LCC, thus producing redundant sources of alarm. This will be possible due to the decentralized architecture of ISNet, which provides several processing nodes, and a redundant communication infrastructure.

It is worth noting that SeismNet Alarm is actually relatively neutral with respect to the underlying seismic network. In fact, it uses the broadly available SeedLink communication protocol to retrieve the seismic data. Furthermore, it can be tailored for different network topologies, alarm thresholds, by altering its configuration files. Of course, this requires a preliminary tuning phase for the target network, achieved by testing the system with real-time and recorded data.

Magnitude estimations

For ISNet, different methods of estimating magnitudes are operative. We have developed a local magnitude scale to provide external general information on the seismicity of the area, and we routinely evaluate the moment magnitude for seismological studies on the source properties of the recorded events. One advantage of the Moment Magnitude scale is that unlike other magnitude scales, it does not saturate at the upper end. That is, there is no particular value beyond which all large earthquakes have about the same magnitude. For magnitudes smaller than about 3, local magnitudes significantly underestimate the moment magnitude (e.g. Deichmann, 2006), due to inaccurate distance attenuation effects and instrumental corrections. Thus, according to the policy established by the USGS (http://earthquake.usgs.gov/aboutus/docs/020204mag_policy.php), when it is available, the moment magnitude is the preferred magnitude estimate for our network.

Finally, for seismic early-warning applications, we have developed a real-time, probabilistic and evolutionary algorithm for estimation of magnitude, which is aimed at predicting the ground-motion intensity at a given target site.

Local Magnitude

The local magnitude scale has been developed from synthetic Wood-Anderson equivalent seismograms, using data recorded by ISNet (Bobbio et al, 2008). Wood-Anderson displacements are synthesized from the waveforms recorded at the ISNet seismic stations, by removing the response curve of the specific

instrument and by filtering according to the high frequency characteristic response of the Wood-Anderson torsion seismograph, with eigenperiod *T=0.8s*, damping factor *0.8* and magnification *V=2800*.

Data coming from horizontal components of short-period instruments and accelerometers of ISNet are initially integrated to provide effective displacement. The scaling law of amplitude, $\log A_0$ with the distance has been calibrated on a dataset of events recorded at the ISNet stations from January 2006 to June 2008, with the constraint that the magnitude of events with maximum amplitude of *1 mm* is *3*, at an epicentral distance of *100 km.* Assuming a scaling with distance with the following functional form:

$$\log A_0 = n \log R + kR + \beta$$

where the logarithmic contribution mainly accounts for the geometrical spreading, while the linear term is referred to the anelastic attenuation. Minimizing the L^2 distance between observed amplitudes and predicted ones, according to the Ricther law, we obtain the following relation that is valid for the southern Apennines:

$$M_L = \log A + 1.79 \log R - 0.58$$

where A is the maximum amplitude, in mm, and R, the hypocentral distance in kilometers.

The local magnitudes of the earthquakes recorded at ISNet are computed as the algebraic means of the magnitude values estimated at each station. Generally, averaging over a larger number of stations (more than five) that explore a broader distance range, the estimated error is about *0.2-0.3* (Bobbio et al., 2008).

Moment Magnitude

The moment magnitude is derived from the estimation of the seismic moment through the non-linear inversion of the S-wave displacement spectra obtained by the spectral analysis of horizontal acceleration and the velocity records at the ISNet stations. Only the stations that have been used for automatic event location

are included in the seismic moment determination. Based on the earthquake location parameters, a window of 5 s bracketing the theoretical S-wave arrival is selected on the horizontal ground velocity and acceleration records. The standard signal processing chain is perfomed using SAC code and it includes: (i) the mean and trend removal; (ii) the application of a cosine-taper; and (iii) a band-pass two-pole, zero-phase shift, and Butterworth filtering in two frequency bands, 1-50 Hz and 0.25-50 Hz, for the acceleration and velocity time series, respectively. The parameters for signal processing were chosen after preliminary tests that were aimed at optimizing the displacement spectral determination from acceleration and velocity records. The Fourier acceleration and velocity spectra are therefore obtained by Fast Fourier transform from which the displacement spectra are obtained by double and single division for the term $(i\omega)$. The spectra obtained are smoothed using a three-point moving window. The displacement spectra of the horizontal components (NS and EW) are combined to build the spectral modulus:

$$\left|D(\omega)\right| = \sqrt{NS(\omega)^2 + EW(\omega)^2}$$

where ω is the angular frequency. The displacement spectra obtained are fitted to a theoretical model having the form (Boatwright,1980):

$$\left|D(\omega)\right| = \frac{\Omega_o}{(1+(\omega/\omega_c)^2} e^{-\frac{\omega t^*}{2}}$$

Where Ω_0 is the low-frequency spectral level related to the seismic moment Mo (Aki and Richards, 1980), $\omega_c = 2\pi f_c$, with f_c the corner frequency and $t^* = \frac{T_S}{Q_S}$ the anelastic attenuation parameter, where T and Q are the S-wave travel-time and quality factor. The parameters Ω_0, f_c and t^* are estimated by the non-linear inversion of displacement spectra, using the Levenberg-Marquardt (Kenneth and Levenberg, 1944) algorithm implemented in GNUPLOT (http://www.gnuplot.info). This allows for best-fit estimations of parameters and related uncertainties. For each station, an estimate of the seismic moment is obtained assuming a homogeneous propagation medium (Aki and Richards,1980):

$$M_o = \frac{4\pi\rho v_S^3 R\Omega_o}{R_{\theta\varphi} F_S}$$

where R is the hypocentral distane, ρ=2700 Kg/m^3 is the medium density, v_S =3000 m/s, $R_{\theta\varphi}$ = 0.62, as the average S-wave radiation pattern, and *Fs*=2, as the free-surface correction factor. The final values of the seismic moment and the uncertainties are computed by averaging the values obtained from acceleration- and velocity-derived displacement spectra at each station analyzed. The average moment magnitude and the standard deviation are obtained by seismic moment estimates using the the relationship:

$$M_W = \frac{2}{3}(\log_{10} M_o - 9.1)$$

where M_o is expressed in N.m (Hanks and Kanamori, 1979). The spectral parameters inferred from the displacement spectrum inversion also allow for the simultaneous determination of the source radius (Brune,1970):

$$(a = \frac{2.34}{2\pi}\frac{v_S}{f_c})$$

and stress drop (Keilis-Borok,1959):

$$(\Delta\sigma = \frac{7}{16}\frac{M_o}{a^3})$$

Early-Warning Magnitude

The real-time and evolutionary algorithm for magnitude estimation is based on a magnitude prediction model and a Bayesian formulation (Lancieri and Zollo, 2008). It is aimed at evaluating the conditional probability density function (PDF) of magnitude as a function of ground motion quantities measured on the early part of the acquired signals.

The predictive models are empirical relationships that correlate the final

event magnitude with the logarithm of quantities measured in the first 2 s to 4 s of recording. In this application, we use the empirical relationship between low-pass filtered, initial P-peak and S-peak displacement amplitudes, and moment magnitude (e.g. Zollo et al, 2006). While the P-wave onset is identified by an automatic picking procedure, the S-wave onset can be estimated from automatic S-picking or from a theoretical prediction based on the hypocentral distance given by the earthquake location. At each time step, progressively refined estimates of magnitude are obtained from the P-peak and S-peak displacement data. Following a Bayesian approach, the magnitude PDF computed at the previous step is used as *a-priori* information.

Generation of the rapid ground-shaking map

In areas characterized by high seismic hazard and exposure, such as the southern Apennines, the generation of strong ground-shaking maps soon after an earthquake is a key tool to identify the areas that have suffered the greatest damage and losses. This information is fundamental for emergency services, loss estimation, and planning of emergency actions by the Civil Protection Authorities.

Ground-shaking maps are usually computed using an appropriate weighting scheme, with interpolation of the peak ground motion recorded at seismic stations with values estimated at a set of points (denoted as phantom or virtual stations) located in areas where data are not available. At phantom stations, the ground-motion parameters, such as PGA and PGV, are estimated using attenuation relationships based on an empirical model of attenuation and a point-like source, which are generally represented by the following formulation:

$$logPGX = a + bM + clog\sqrt{R^2 + h^2} \pm \sigma_{logPGX} \qquad (1)$$

where *PGX* is the selected strong ground motion parameter (PGA or PGV), *M* is the magnitude, *R* is a distance, *h* the depth of the hypocenter, and σ_{logPGx} is the standard error. The coefficients *a*, *b* and *c* have to be retrieved specifically for each region. For the southern Apennines region, using the available seismological data an *ad-hoc* attenuation relation has been deduced (Convertito el al., 2007). The coefficients obtained for formula (1) are reported in Table I.

Using an attenuation relationship like formula (1), the predicted strong-motion field is isotropic around the epicentral area, while the observed field shows a bi-dimensional distribution that depends upon both source-to-site distance and the azimuth caused by fault geometry, focal mechanism, and directivity effects. These effects are partially accounted for in a different way by the existing techniques adopted for ground-shaking map computation. For example, to account for the fault geometry, ShakeMap (Wald et al., 1999a) uses a schematic representation of the fault, i.e. a box representing the surface fault projection, and uses the minimum fault distance definition instead of the epicentral distance.

Taking advantage of ISNet, a tool for the rapid estimation of ground-shaking maps after moderate-to-large earthquakes has been developed (Convertito at al, 2008). Named as GRSmap, its main features include:

- The determination of peak parameters at phantom stations using observed and predicted data at the same time, by the attenuation relationship reported in Table I. In this way, the azimuthal properties of the recorded peak-ground-motion field are preserved.
- The automatic choice of the parameters controlling the distribution of the phantom stations, mainly based on the density of the seismic network.

This is obtained by dividing the area where the ground-shaking map has been calculated into two zones: the area covered by the seismic network, denoted as the data domain, and the external area to the seismic network. Different techniques are then used in these two cases, both to define the location of the phantom stations and to correct the estimated ground-motion values, to bring them into line with the observations that implicitly contain source and propagation effects. In the data domain, a triangulation scheme is used to obtain a uniform distribution of stations covering the area of interest, while in the external area, a regular grid of phantom stations is used.

The methodology used to develop the GRSmap software can be schematically summarized as follow:

Triangulation of the data domain:

- Recorded PGA and PGV values are reported to rock-site conditions using *ad-hoc* corrective coefficients obtained using the same approach as proposed by Borcherdt (1994) and Park and Ellrick (1998), and as retrieved by Cantore et al. (2008).
- The seismic stations correspond to the vertices of the triangles. For each triangle, the barycenter is identified and used as a phantom seismic station.
- The area of each triangle cannot exceed $N_A \times A_{ave}$, where N_A is an integer that depends on the density of the seismic network, and A_{ave} is the average area of all of the triangles. The triangles with areas exceeding the fixed threshold are recursively triangulated using the new barycenters as additional vertices. At all of the new barycenters the ground-motion parameters are assigned using the adopted attenuation relationships corrected by the average residual calculated on a fixed number of real seismic stations.
- The epicenter is considered as an additional station where the peak ground-motion values are estimated using the attenuation relationship at R = 0 km. A correction is then applied, corresponding to an average residual computed at a number of stations surrounding the epicenter below a critical distance value (d_c) that depends on the seismic network density.
- For earthquakes located outside of the data domain area, triangulation of the epicentral area is made denser and denser until a uniform station distribution is obtained.

Ground-motion-residual estimation:

- Given the optimal triangulation, the residuals are calculated at each vertex of the triangles by comparing the observed and the predicted ground-motion values obtained by the attenuation relationship proposed by Convertito et al. (2007) (see Table I). The average residual is then used to correct the predicted value at each barycenter.

  Once the earthquake location and magnitude have been fixed, the attenuation relationship is used to obtain theoretical estimates at the network recording sites. Considering the *i*-th triangle (Fig. 5, inset, panel a), the vertices of which are labelled as P_1, P_2 and P_3, the peak motion residual term at the *j*-th vertex is computed as the difference between the

observed and the estimated peak-ground motion. The maximum acceptable residual value is fixed on the basis of the estimated fault length (L), obtained by using the Wells and Coppersmith (1994) relationships, and an epicentral area is defined by a circle of radius L/2 centered on the epicenter (panel a in Fig.5). The residuals cannot exceed $N\sigma_{logPGX}$, where σ_{logPGX} is the standard error of the selected attenuation relationship. The value of N is generally fixed at 4 for sites located inside the epicentral area, and otherwise at 3. If a single residual is outside the fixed range, the datum is considered as an outlier and is not used in the map computation. Otherwise, for a given triangle, the average peak-motion-residual term is then obtained and used to estimate the peak-motion amplitude at the *i*-th barycenter point B_i. The procedure is repeated for all of the triangles and iterated until a uniform coverage of the data domain area is obtained. This allows for a local correction, which accounts for azimuthal variations due to source effects, like directivity and focal mechanisms.

Extrapolation of peak motion in the external area

For the area not covered by the seismic network, the first problem is the definition of the optimal grid spacing of the phantom stations. Another problem is represented by the definition of the threshold distance to the closest station where recorded data are available. This distance provides an empirical measure of the extent to which the observed data can be extrapolated outside the data domain area. In the proposed technique, the external area is covered with a uniform grid of phantom stations, the spacing interval of which is fixed to a fraction of the average distance between the stations and barycenters. The same value is used for the threshold distance (αd_c) (Fig. 5, panel a).

Among all of the nodes of the grid, only those located at distances greater than the threshold value from the closest recording station are retained (Fig. 5, circles). At each retained node, the peak ground-motion parameter is then predicted using the attenuation relationship, adding a mean residual weighted for the epicentral distance, computed at seismic stations with an azimuth with respect to the epicenter, comparable with that of the phantom station considered.

The estimated and recorded data are than integrated and used to generate the ground-shaking map by re-interpolating onto a finer regular grid that is

uniformly spaced at an arbitrary spacing interval of 0.01 degree. This map is finally corrected for site effects using the corresponding corrective coefficients (Cantore et al., 2008).

Application to the 23 November, 1980, Irpinia earthquake (M 6.9)

The GRSmap software has been applied to compute ground-shaking maps of the last destructive earthquake that occurred in the southern Apennines: the 23 November, 1980, Irpina M 6.9 earthquake. This was characterized by a complex normal faulting that ruptured three different sub-parallel fault segments of the southern Apennine belt chain (Westaway and Jackson, 1984; Bernard and Zollo, 1989). The parameters of the three faults are listed in Table 2. Figure 5 shows the location of the accelerometers (triangles) of the local seismic network managed by ENEA-ENEL (Berardi et al., 1981) at which data were available, and the instrumental epicenter (grey star). The phantom stations (circles), the triangulation scheme, and the barycenters (black dots) are also shown in Figure 5. The average area of the triangles is about 473 km^2, while the threshold distance and phantom spacing of the grid is about 62 km.

To highlight the advantages of the technique proposed in the present study, the ground-shaking maps were calculated using a version of the attenuation relationships obtained by excluding the data of the Irpinia earthquake from the dataset (Table I). The computed ground-shaking maps are shown in Figure 6. In particular, Figure 6a shows the PGA maps expressed as percentages of the gravity acceleration, Figure 6b shows the PGV map expressed in cm/s, and Figure 6c shows the map of the instrumental intensity.

Note that although the predictive attenuation model was based on the assumption of a point-like source, the maps reproduce the extension of the three fault segments and the associated complex ground-motion pattern. This can be attributed to the use of recorded data and corrected estimates at the barycenters that provide improved coverage of the source area. Both the PGA and PGV maps reproduce the directivity effect, which is towards the north-west for fault segment F1 and towards the south-east for fault segment F2, and which is characterized by the larger ground-motion values in those directions. Furthermore, as a result of using the weighted average scheme proposed by Wald et al. (1999b) to convert

PGA and PGV into instrumental intensities, the instrumental intensity map is directly connected to the PGA and PGV maps.

Software for the hardware and data management

To manage all of the hardware comprising ISNet, the software systems that are running and the data produced by the network, we have developed a custom application: SeismNet Manager. This application acts as a high level, web-based graphical front-end to the network, for internal full management of ISNet, as well as for external users who are interested in the seismological data acquired.

SeismNet Manager provides an instrumental and seismological database to keep track of the hardware components that comprise the network, and of the data they produce. The application fulfills the following needs:

- to keep an inventory and to store the details of the components that constitute a seismic network, including: station sites, sensors, loggers, communication and generic hardware, and servers;
- to keep a history of the installations and configurations of these components, and of their mutual connections;
- to perform real-time monitoring of the devices: retrieving their internal variables, and detecting "health" problems and assessing the quality of their output, thus producing alarms and information that complement the seismic data;
- to manage the seismic data produced by the network. These data are either automatically retrieved, e.g. events from bulletins, automatically detected events, and related waveforms, or manually inserted by the researchers, e.g. arrival times, alternative event magnitudes and locations, and focal mechanisms;
- to perform some routine tasks on the seismic data, such as inspection, filtering, picking and flagging;
- to offer a graphical, web-based interface to the staff of the network for inserting, editing, searching, downloading and displaying all of this information (as tables, graphs, maps, waveform plots, 3D renderings).

SeismNet Manager is implemented through open technological components, and can roughly be broken down into these main components:

- the web application, that provides the user interface, controls the hardware monitoring, and offers various tools to edit and display data. It is composed of *JavaServer Pages* code (run by Apache Tomcat [1]), and Java programs and applets;
- a relational database for both instrumental and seismic data, implemented in *PostgreSQL* [2];
- several small programs, written in various languages, called *agents*. Each agent is in charge of communicating with a different type of hardware that is deployed as part of the network. The real-time hardware monitoring is implemented through this *plug-ins* based approach;
- procedures for the automatic acquisition of waveform data, from heterogeneous data sources such as logger disks, Earthworm servers, and FTP servers.

In the following paragraphs the management of the hardware forming ISNet is initially described, followed by the management of the data produced.

Hardware Management

Through SeismNet Manager, it is possible to create a new object belonging to one of several hardware types (e.g. logger, sensor, server) and to fill in the details of that physical object. Some details are common to any hardware type, e.g. model name, serial number, inventory number, vendor name. Other fields are specific to each class of object e.g. number of channels of a data logger, physical quantity recorded by a sensor. It is then possible to create stations and LCCs, and communication lines between them, and to install devices at each site. A hardware-specific configuration corresponds to each installed device, and a series of connections with other nearby devices. A database of the entities mentioned, each valid from a start date to an optional end date, records all of the details of the ISNet hardware at any instant in time.

[1] http://tomcat.apache.org
[2] http://www.postgresql.org

To complement this "static" knowledge that is manually entered by the administrators of the network, there exists a hardware monitoring layer, which analyzes the internal state and working conditions of the hardware. Devices with an IP address, such as loggers, servers and communication hardware, are routinely queried for their most significant internal variables, to identify "health" problems. Typical variables are the power supply voltage of a device or its internal temperature, the disk space in a server, or the data-flow parameters from a logger.

The queried variables, as well as the communication protocol, in general depend on the hardware type (and brand). For this reason, the interrogations are carried out by several apposite external programs called *agents*, one for each hardware class. The hardware monitoring is configured by choosing the target devices, the agents to be used with them, and the starting times and frequencies of the interrogations. Additionally, each station features a programmable GSM phone terminal that is connected to several environmental sensors in the shelter, e.g. the door, batteries level, smoke sensor. This sends a text message whenever one of the thresholds is met.

All of the internal variables and the gathered information on the state of the instrumentation are stored in the database, and can be shown as tables or graphed directly in the browser.

The front page of SeismNet Manager (figure 7) is meant to convey the state of the whole network at a glance. It consists of a map with stations, LCCs, and communication lines. Overlaid on each station are: a color-coded overall state; the installed sensors and their working conditions; icons for any problem detected by the hardware monitoring agents or messages sent by the station.

Events, waveforms and seismic data

SeismNet Manager contains a seismological database that keeps track of the seismic events detected by the network, with the associated metadata and waveforms recorded by the sensors. The main source of events is the automatic earthquakes detection system that runs at each LCC, implemented in Earthworm. Upon detecting an event, the earthquake metadata (location, magnitude estimation, focal mechanism) is sent to SeismNet Manager. For events that are not automatically detected, such as regional and teleseismic ones, SeismNet Manager

makes use of alert messages and bulletins produced by national and international seismological agencies.

New events signaled to SeismNet Manager are first tested against some rather conservative magnitude and distance thresholds, to filter out too distant or too weak earthquakes. Then the procedures for automatic waveform data retrieval from the stations are activated. These procedures exploit several waveforms sources (e.g. Earthworm servers, mass storage in the data loggers, FTP servers with manually obtained data) to retrieve the sensor signals, in a time window that includes the expected recording of the event at each site. To determine the seismic stations and time window to retrieve data from, the procedures take into account: the sensor type (e.g. only broad-band sensors for teleseismic events); the P-wave arrival time at each station, estimated using the IASPEI travel-time tables [3] for regional and teleseismic events, or a custom velocity model for local events; the earthquake time length duration, computed through a regression law between magnitude and duration (for local and regional events), or other criteria based on distance and magnitude (teleseisms).

Each waveform entering the system is converted into a uniform file format. We chose the SAC [4] file format (Seismic Analysis Code, from Lawrence Livermore National Laboratory), with the file header filled with the details of the associated event, the estimated arrival time, the originating site and instruments that recorded the data. A data quality parameter is also assigned to each waveform, automatically computer-evaluating the signal to noise ratio of the signal level of the recorded earthquake compared to the noise level before the event. Users can then search events and waveforms by defining multiple search criteria on a web page (figure 8). Events can be filtered for time and location, magnitude value and type, and epicentral distance. Waveforms can be filtered for station, sensor type and model, and component and quality. Waveforms recorded by a sensor flagged as having issues can be filtered out. Additionally, it is possible to filter out all of the three components from a sensor, whenever even a single component has a quality below that requested.

The waveforms matching the search criteria, and the associated metadata, can be downloaded as a compressed archive, or viewed and manipulated through

[3] http://www.iris.edu/pub/programs/iaspei-tau
[4] http://www.iris.edu/software/sac

the *SeisGram2K* [5] Java applet (figure 9). The matching events can be rendered as an interactive 3D scene, using a browser plug-in for VRML (Virtual Reality Modeling Language) Files (figure 9). All of the data associated with a seismic event can be displayed and edited through either web pages or java applets. In a typical session, a logged in user will:

- display the waveforms associated to a seismic event with SeisGram2K, including the estimated arrival times, as computed when the waveform was inserted;
- manually revise these picks;
- submit changes to the system (by clicking a button). This will automatically compute a new earthquake location, magnitude, and focal mechanism. The system retains the previous values and keeps track of the author and timestamp of each change, making it easy to choose among several authors, or to revert to previous solutions.

A demonstration tour of SismNetManager can be found here:
http://dbserver.ov.ingv.it:8080

Discussion and conclusions

The system presented here has been developed in the framework of an ongoing project financed by the Regional Department of Civil Protection, with the idea that Regione Campania can be considered as a potential EEWS target-site for experimenting innovative technologies for acquisition, rapid processing, management and diffusion of data based on ISNet. Indeed, with about six million inhabitants and a large number of industrial plants, the Campania Region (southern Italy) is a zone of high seismic risk due to moderate to large magnitude earthquakes on active fault systems in the Apennine belt. Considering an earthquake warning window ranging from tens of seconds before to hundred of seconds after an earthquake, many public infrastructures and buildings of strategic relevance (hospitals, gas pipelines, railways, railroads) in the Regione Campania can be considered as potential EEWS target-sites for experimenting innovative technologies for data acquisition, processing and transmission, based on ISNet.

[5] http://alomax.free.fr/seisgram/SeisGram2K.html

The expected time delay to these targets for the first energetic S-wave train is more than 20 s at about 100 km from a crustal earthquake occurring in the source region.

At present, several EEWS have been implemented worldwide. In Japan, since 1965, the JNR (Japanese National Railways) has developing and is operating the Urgent Earthquake Detection and Alarm System (UrEDAS) system, which is an on-site warning system along the Shinkansen railway. UrEDAS is based on seismic stations deployed along the Japanese Railway at average distances of 20 km, and an alert is issued if the horizontal ground acceleration exceeds 40 cm/s^2 (Nakamura, 2004). Furthermore, an innovative EEWS started nationwide in Japan at the end of 2007, managed by the Japan Meteorological Agency (JMA) using data from more than 1,000 seismic stations (Hoshiba et al., 2008). After a quick determination of the hypocenter and magnitude using records from the closest stations, a predicted arrival time of shear waves is provided for districts where the seismic intensity is predicted to be equal to 4 or more on the JMA scale. A step-by-step procedure is adopted to improve the accuracy of the estimation as the available data increase with elapsed time. The information are automatically disseminated by the JMA to the final users, who are classified as limited or general users. The limited users are organizations (railway companies, elevator companies, manufacturing industries) who can carry out an automatic check of their system. For the general users, the earthquake early-warning alarms are provided by various means, such as television, radio, cellular phone and the Internet (Hoshiba et al., 2008).

In Taiwan**,** the Taiwan Central Weather Bureau (CWB) has developed an early-warning system based on a seismic network consisting of 79 strong-motion stations (Wu and Teng, 2002). Since 1995, the network has been able to report event information (location, size, strong-motion map) within 1 min of the earthquake occurrence (Teng et al. 1997). To reduce the reporting time, Wu and Teng (2002) introduced the concept of a virtual sub-network: as soon as an event is triggered by at least seven stations, the signals coming from the stations that are less then 60 km distant from the estimated epicenter are used to characterize the event. This system was operating from December 2000 to June 2001 (7 months), and it successfully characterized all of the 54 events that occurred, with an average reporting time of 22 s.

Other systems are under development in Mexico, Turkey, Romania and California. An extended review of the existing early-warning systems is reported in a special volume of "Seismic Early Warning", edited by Gasparini et al. (2006), and by the study of Zollo et al. (2008a).

However, how can it be verified whether an EEWS is functioning correctly? The main test would be to wait until a significant number of earthquakes have been recorded, also of medium to large energy, and to verify the number of alarms that have correctly been sent, along with the number of false alarms and alarms missed. Moreover, it is necessary to verify the significance of each alarm, including the useful time before the arrival of the destructive seismic wave, and the predicted amplitude at a site with respect to that which is actually recorded. For instance, the EEWS operating in Japan by JMA was tested for 29 months, starting in February 2004. During this period, the JMA sent out 855 earthquake early warnings, with only 26 recognized as false alarms due technical problems or human error (Hoshiba et al., 2008).

For the area of the southern Apennines, because of the scarcity of relatively large earthquakes, this means that it is difficult to experimentally test this EEWS based on ISNet. Many tests have been performed using low energy earthquakes, with magnitudes of about 3, but we believe these tests are actually not fully significant. Therefore, we have decided to use synthetic seismograms that have been computed at all of the recording sites of our seismic network to evaluate the performance of the implemented EEWS. We have considered several cases of earthquakes of M 6 and M 7 occurring inside or at the border of ISNet, and we have performed a massive computation of seismograms for a large number of characteristic earthquake scenarios (Zollo et al., 2008b). By using the computational methodologies previously described, we have retrieved early estimates of source parameters and we have predicted the peak ground motions (PGA, PGV) at selected sites. In this way, we have investigated the system performances in cases of complex, extended rupture processes, and the seismic source characteristics such as directivity, rupture velocity distribution and near-field contributions have been considered. Two parameters are used to define the system performance: Effective Lead Time (ELT), i.e. the time at which the probability of observing the true PGV, within one standard deviation, becomes stationary; and the Probability of Prediction Error (PPE), which provides a

measure of the PGV prediction error. The geographical distribution of ELT and PPE for the southern Apennines shows a significant variability up to large distances around the fault, thus indicating that the ability of the system to accurately predict the observed peak ground motions strongly depends on the distance and azimuth from the fault. Assuming an earthquake with similar source characteristics to that of the November, 1980, Ms=6.9 earthquake for the metropolitan area of Naples (see Figure 1), the ELT ranges between 8 s and 16 s, and the PPE between 50% and 60%, indicating that several mitigation actions could be effective before S-waves shake the town (Zollo et al, 2008b).

ISNet is thus set up to acquire strong-motion records of large earthquakes near to their source, along with very low magnitude local events, and records of distant earthquakes (teleseisms). The data recorded are inserted into our database, which now comprises more than 1,050 events with $0.1 \leq ML \leq 3.0$, with more than 23,000 three-component traces. This dataset grows at the rate of about 30-35 events with an $ML \leq 3$ per month, providing us with an outstanding tool for the analysis of the microseismicity in the area.

AVAILABILITY OF DATA

All of the seismic waveform data archived by the ISNet-Irpinia Seismic Network are available upon request directly at info@isnet.amracenter.com. Alternatively, waveform data can be retrieved from the SeismNetManager (SAC format). To access SeismNet Manager, it is necessary to register an account and to authenticate this first. The form to request access to the ISNet data can be found at the following address: http://dbserver.ov.ingv.it:8080.

References

Aki K, Richards P (1980) Quantitative Seismology, Theory and Methods, vols. I and II
WH Freeman, New York

Berardi RA, Berenzi, Capozza F (1981) Campania-Lucania earthquake on 23 November 1980: accelerometric recordings of the main quake and relating processing. Technical report Ente Nazionale per l'Energia Elettrica (ENEL), Rome

Bernard P, Zollo A (1989) The Irpinia (Italy) 1980 earthquake: detailed analysis of a complex normal fault. J Geophys Res 94:1631-1648

Bobbio A, Vassallo M, Festa G (2008) A Local Magnitude Scale for the Southern Italy. Bull Seismol Soc Am, submitted.

Borcherdt RD (1994) Estimates of site-dependent response spectra for design (methodology and justification). Earthquake Spectra 10:617-654

Boschi E, Gasperini P, Mulargia F (1995) Forecasting Where Larger Crustal Earthquakes Are Likely to Occur in Italy in the near future. Bull Seismol Soc Am, 85:1475-1482

Brune JN (1970) Tectonic stress and the spectra of seismic shear waves from earthquakes. J Geophys Res 75:4997-5009

Cantore L, Convertito V, Zollo A, Elia L (2008) Site-condition map and site amplification corrections for early-warning applications and seismic hazard assessment in the Campania-Lucania Region (southern Apennines), Italy, in preparation

Cinti, F R, L Faenza, W Marzocchi, P. Montone (2004), Probability map of the next M 5.5 earthquakes in Italy, Geochem. Geophys. Geosyst., **5**, Q11003, doi:10.1029/2004GC000724

Chiarabba C, Amato A. (1996) Crustal velocity structure of the Apennines (Italy) from P-wave travel time tomography. Annali di Geofisica, 34, N.6, 1133-1148.

Convertito V, De Matteis R, Romeo A, Zollo A, Iannaccone G (2007) Strong motion relation for early-warning applications in the Campania Region (southern Apennines), Italy. In Gasparini et al (eds) Earthquake early warning systems, Berlino, Springer-Verlag.

Convertito V, De Matteis R, Zollo A Iannaccone G (2008) Rapid ground motion prediction for emergency management in the Campania-Lucania region, Southern Italy by using ISNet seismic network. Natural hazards, in press.

Deichmann N (2006) Local Magnitude, a Moment Revisited. Bull Seismol Soc Am 96:1267-1277

Gasparini P, Manfredi G, Zschau J (2006) Earthquake early warning systems, Berlino, Springer-Verlag.

Hanka W, Heinloo A, Jaeckel K (2001) Networked Seismographs: GEOFON Real-Time Data Distribution, OHP/ION symposium "Long-Term Observations in the Oceans: Current Status and Perspectives for the Future", Mt. Fuji, Japan, January 21 - 27, 2001.

Hanks TC, Kanamori H (1979) A moment magnitude scale. J Geophys Res 84: 2348–2350

Hoshiba M, Kamigaichi O, Saito M, Tsukada S, Hamada N (2008), Earthquake Early Warning Starts Nationwide in Japan. Eos Trans. Vol.89, 8, 73-80

IASPEI new manual of seismological observatories practice (NMSOP) (2002). Ed. Peter Bormann, Geoforschungs Zentrum Postdam.

Improta L, Iannaccone G, Capuano P, Zollo A, Scandone P (2000) Inferences on the upper crustal structure of Southern Apennines (Italy) from seismic refraction investigations and subsurface data. Tectonophysics, 317, 273-297.

Improta L, Bonagura MT, Capuano P, Iannaccone G (2003) An integrated geophysical investigation of the upper crust in the epicentral area of the 1980, M_s=6.9, Irpinia earthquake (Southern Italy). Tectonophysics 361: 139-169.

Johnson CE, Bittenbinder A, Bogaert B, Dietz L, Kohler W (1995) Earthworm: A flexible approach to seismic network processing. IRIS Newsletter 14(2), 1-4.

Keilis-Borok V (1959) On the estimation of the displacement in an earthquake source and of source dimensions. Ann. di Geofisica 12:205-214

Kenneth Levenberg (1944) A Method for the Solution of Certain Non-Linear Problems in Least Squares. The Quarterly of Applied Mathematics 2: 164–168.

Lancieri, M, Zollo A (2008) A Bayesian approach to the real-time estimation of magnitude from the early *P* and *S* wave displacement peaks. J. Geophys. Res. 113- B12302

Nakamura Y (2004) Uredas, Urgent Earthquake Detection and Alarm System, Now and Future 13th World Conference on Earthquake Engineering 908

Pantosti D and Valensise G (1990) Faulting mechanism and complexity of the 23 November, 1980, Campania-Lucania earthquake inferred form surface observations, J. Geophys. Res. 95:319-341

Park S, Elrick S (1998) Predictions of shear wave velocities in southern California using surface geology. Bull Seismol Soc Am 88:677-685

Reiter L (1990) Earthquake hazard analysis - issues and insights. Columbia University Press, New York, 254 pp.

Richter C (1935) An instrumental earthquake magnitude scale. Bull Seismol Soc Am 25:1-32.

Satriano C, Lomax A, Zollo A (2008) Real-Time Evolutionary Earthquake Location for Seismic Early Warning. Bull Seismol Soc Am 98:1482-1494

Teng, T. L., Y-M. Wu, , T. C. Shin, Y.B. Tsai and W.H.K. Lee (1997) One minute after: strong-motion map, effective epicenter, and effective magnitude. *Bull. Seism. Soc. Am., 87*, 1209-1219.

Wald DJ, Quitoriano V, Heaton TH, Kanamori H, Scrivner CW, Worden CB (1999a) TriNet shakemaps: rapid generation of instrumental ground motion and intensity maps for earthquakes in southern California. Earthquake Spectra 15:537-555.

Wald DJ, Quitoriano V, Heaton TH, Kanamori H (1999b) Relationship between peak ground acceleration, peak ground velocity, and modified Mercalli intensity for earthquakes in California. Earthquake Spectra 15:557-564.

Westaway RWC, Jackson J (1984) Surface faulting in the southern Italian Campania-Basilicata earthquake of 23 November 1980. Nature 312:436-438.

Weber E, Convertito V, Iannaccone G, Zollo A, Bobbio A, Cantore L, Corciulo M, Di Crosta M, Elia L, Martino C, Romeo A, Satriano C (2007) An advanced seismic network in the southern Apennines (Italy) for seismicity investigations and experimentation with earthquake early warning: Seismological Research Letters 78, 622-534

Wells DL, Coppersmith KJ (1994) New empirical relationships among magnitude, rupture length, rupture width, rupture area, and surface displacement. Bull Seismol Soc Am 84:974-1002.

Wu Y-M and Teng T (2002) A virtual subnet approach to earthquake early warning. Bull Seismol Soc Am 92, 2008-2018

Zollo A, Lancieri M, Nielsen S (2006) Earthquake magnitude estimation from peak amplitudes of very early seismic signals on strong motion records. Geophysical Research Letters 33- L23312

Zollo A., Iannaccone G., Convertito V., Elia L., Iervolino I., Lancieri M., Lomax A., Martino C., Satriano C., Weber E. and Gasparini P., (2008a), The Earthquake Early Warning System in Southern Italy. *Encyclopedia of Complexity and System Science - Springer Verlag.*

A.Zollo A, Iannaccone G, Lancieri M, Cantore L, Convertito V, Emolo A, Festa G, Gallovic F, Vassallo M, Martino C, Satriano C and Gasparin P (2008b) The Earthquake Early Warning System in Southern Italy : Methodologies and Performance Evaluation, submitted to Geophysical Research Letters

Tables

Pgx	*a*	*b*	*c*	*h*	σ
Pga (m/s^2)	-0.559	0.383	-1.4	5.5	0.155
Pgv (m/s)	-3.04	0.552	-1.4	5.0	0.154
Pga (m/s^2)[a]	-0.514	0.347	-1.4	5.5	0.145
Pgv (m/s)[a]	-3.13	0.570	-1.4	5.0	0.185

Table 1: Regression coefficients and standard errors of the regional attenuation relationship used to compute the ground-shaking maps (Convertito et al., 2007). The superscript a indicates the coefficients of the same attenuation relationships obtained without introducing the PGA and PGV values of the 23 November 1980 Irpinia earthquake into the dataset.

Parameter	***F1***	***F2***	***F3***
Length	35 km	20 km	20 km
Width	15 km	15 km	10 km
Depth of the top	2.2 km	10 km	2.2 km
Strike	315°	300°	124°
Dip	60°	20°	70°
Slip	-90°	-90°	-90°
Seismic moment	2×10^{19} Nm	4×10^{18} Nm	3×10^{18} Nm

Table 2: Fault parameters of the 23 November 1980 Irpinia earthquake (after Bernard and Zollo, 1989)

FIGURES:

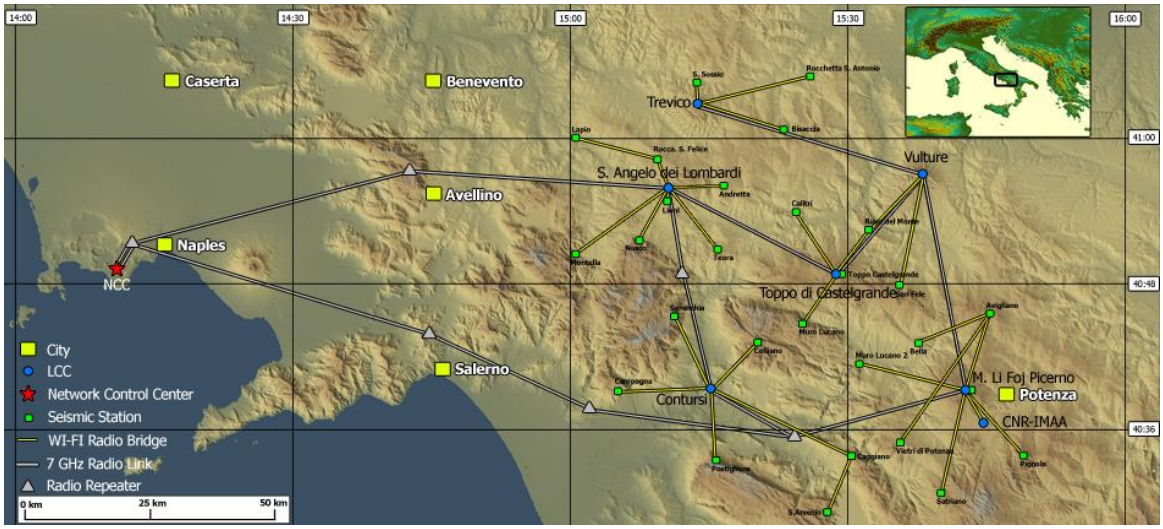

Figure 1: The ISNet network in Campania-Lucania Apennine (Southern Italy). Green squares indicate seismic stations. Yellow lines symbolize wireless radio links between each seismic station and its nearest Local Control Center (LCC, blue circles). Gray lines represent higher bandwidth, wireless connections among LCCs and the Network Control Center (red star). The latter transmission system is conceived as a redundant double ring.

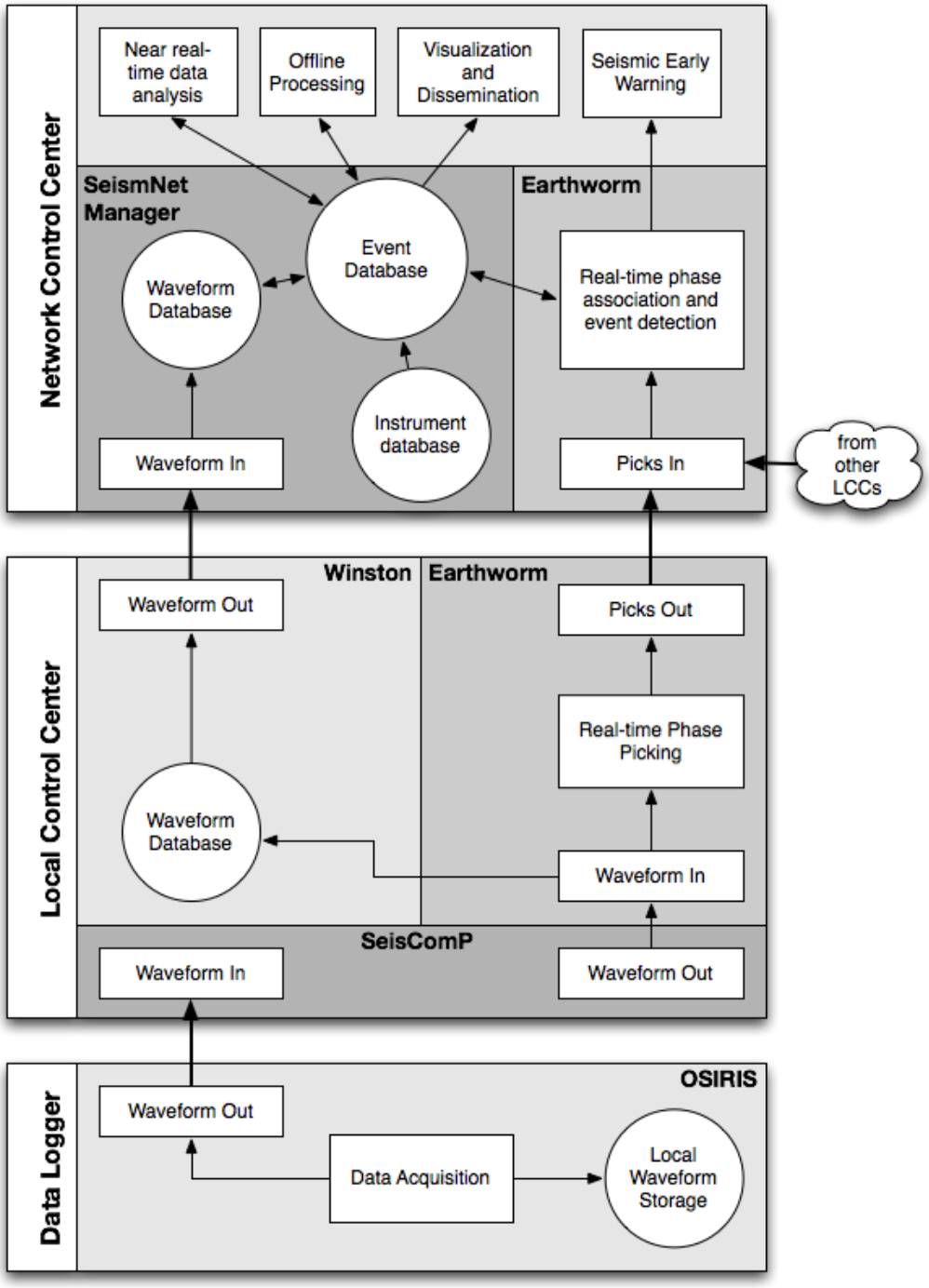

Figure 2: Real-Time data management at the ISNet is organized into three logical layers, which follow the physical structure of the network. The base layer is the data-logger, where the ground motion signal is digitized, time stamped and sent over a network connection. The middle layer is the Local Control Center (LCC) where real-time analysis is performed on data from the attached stations. Furthermore each LCC maintains a waveform database for local stations. The top layer is the Network Control Center (NCC), where phase association and event detection is performed and where the network-wide database is kept. Also the NCC provides facilities for other applications (seismic early warning, near-real time processing, etc.) and for end users.

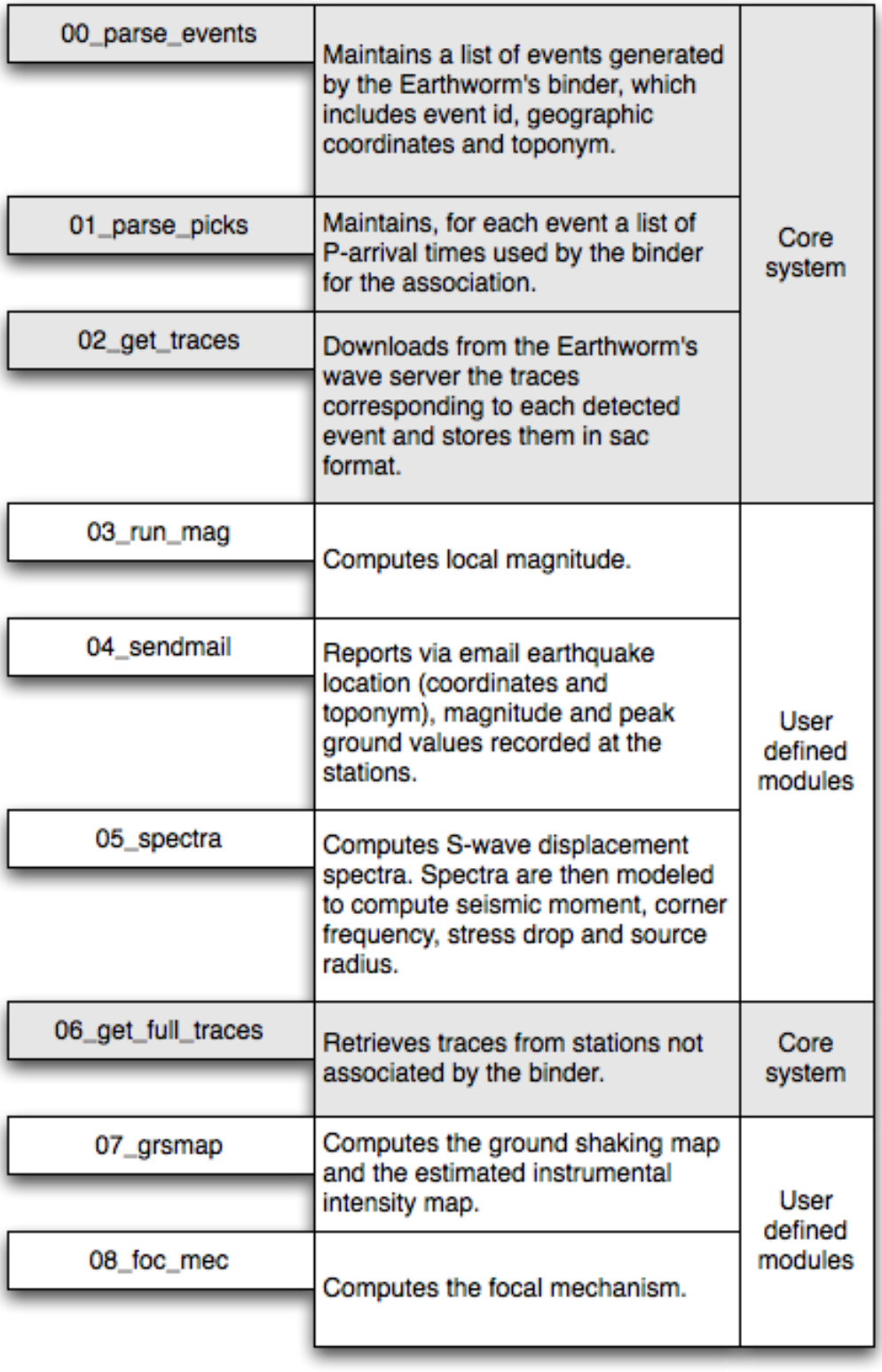

Figure 3: Scheme of the near real-time analysis procedure at the ISNet. The procedure is organized as a chain where each module is activated after the previous one. The whole chain is run every 2 minutes; several chains can run in parallel. The modules are logically divided into two families: "Core system", which comprises modules that interact with the underlying Earthworm system, and "User defined modules".

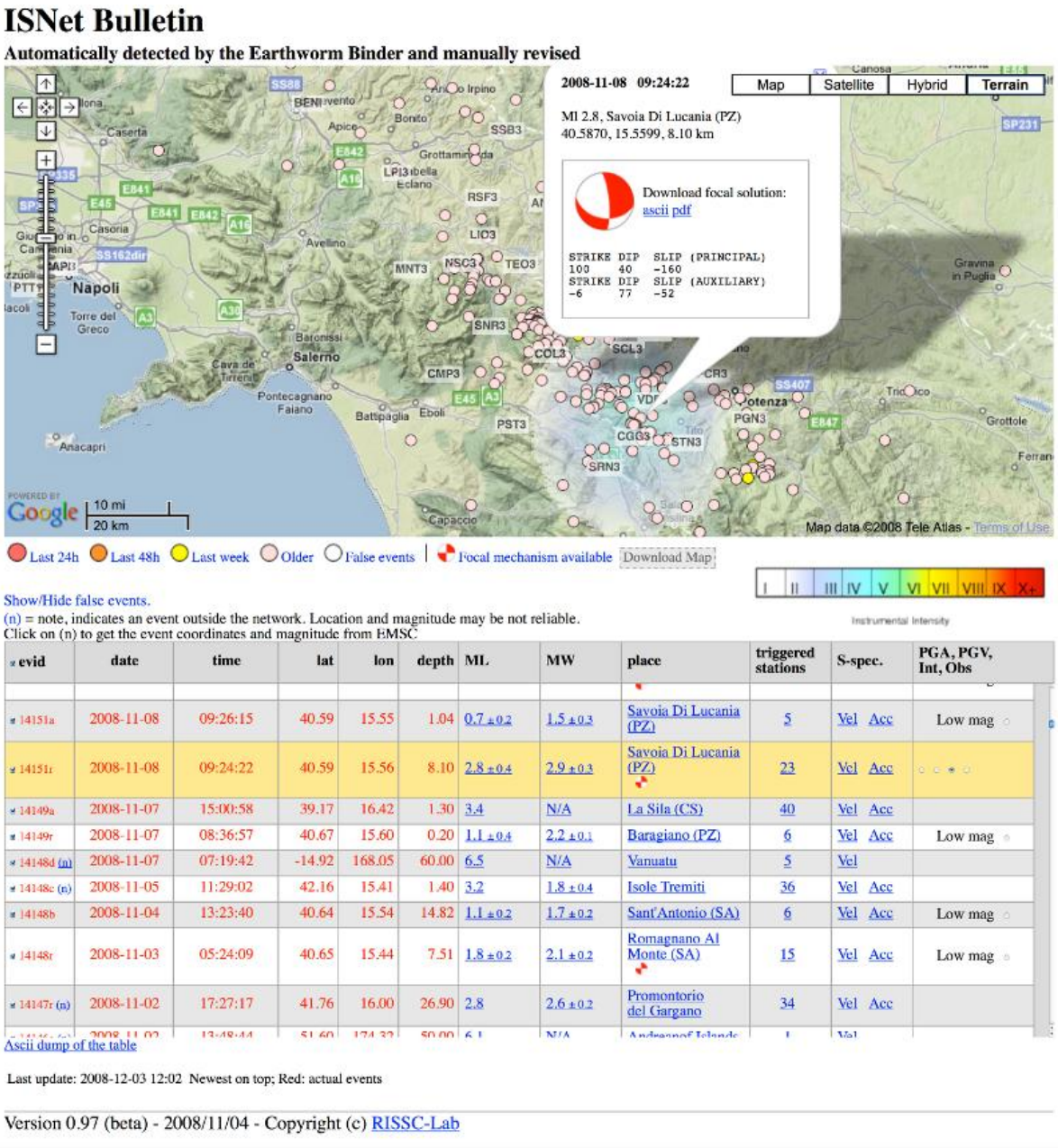

evid	date	time	lat	lon	depth	ML	MW	place	triggered stations	S-spec.	PGA, PGV, Int, Obs
14151a	2008-11-08	09:26:15	40.59	15.55	1.04	0.7 ± 0.2	1.5 ± 0.3	Savoia Di Lucania (PZ)	5	Vel Acc	Low mag
14151r	2008-11-08	09:24:22	40.59	15.56	8.10	2.8 ± 0.4	2.9 ± 0.3	Savoia Di Lucania (PZ)	23	Vel Acc	
14149a	2008-11-07	15:00:58	39.17	16.42	1.30	3.4	N/A	La Sila (CS)	40	Vel Acc	
14149r	2008-11-07	08:36:57	40.67	15.60	0.20	1.1 ± 0.4	2.2 ± 0.1	Baragiano (PZ)	6	Vel Acc	Low mag
14148d (n)	2008-11-07	07:19:42	-14.92	168.05	60.00	6.5	N/A	Vanuatu	5	Vel	
14148c (n)	2008-11-05	11:29:02	42.16	15.41	1.40	3.2	1.8 ± 0.4	Isole Tremiti	36	Vel Acc	
14148b	2008-11-04	13:23:40	40.64	15.54	14.82	1.1 ± 0.2	1.7 ± 0.2	Sant'Antonio (SA)	6	Vel Acc	Low mag
14148r	2008-11-03	05:24:09	40.65	15.44	7.51	1.8 ± 0.2	2.1 ± 0.2	Romagnano Al Monte (SA)	15	Vel Acc	Low mag
14147r (n)	2008-11-02	17:27:17	41.76	16.00	26.90	2.8	2.6 ± 0.2	Promontorio del Gargano	34	Vel Acc	

Figure 4: The "ISNet Bulletin" interactive web page. Circles in the Google map on the upper half of the page represent events detected by the system. The events, with the associated parameters, are reported in the interactive table on the second half of the page. Additional information for each event is reported in the map or in a pop-up page by simply clicking on one or more parameters of the event. As an example, the instrumental intensity and the detailed information, including focal mechanism, for a ML=2.8 event are displayed.

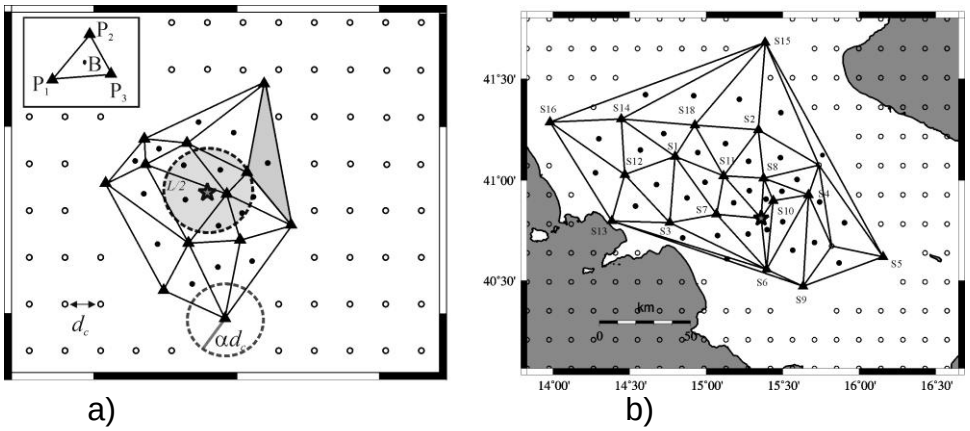

Figure 5: (a) Schematic representation of the main parameters used to triangulate the data domain area and to cover the area external to the seismic network. (b) Location of the stations of ENEL-ENEA network and triangulation scheme used to compute the ground shaking map of the 23 November 1980 Irpinia earthquake.

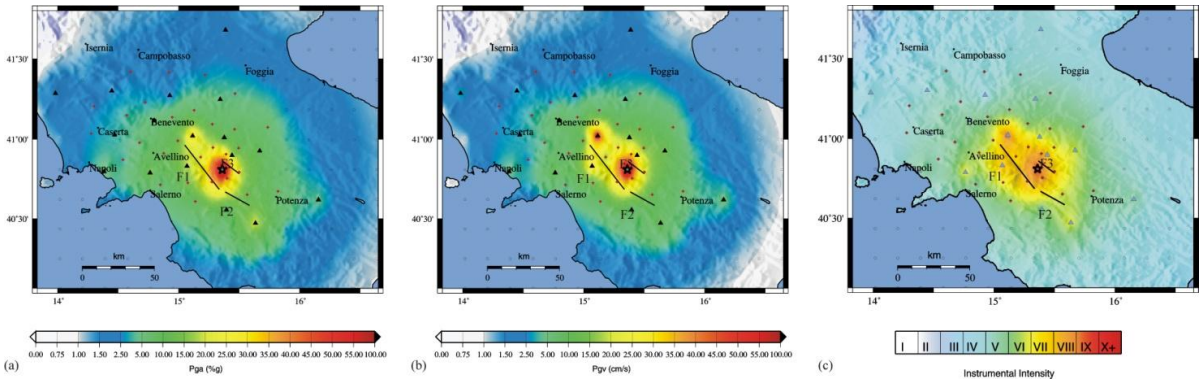

Figure 6: Ground shaking maps of the 23 November 1980 (M 6.9) Irpinia earthquake. Panel (a) shows the ap of PGA, panel (b) shows the map of PGV and panel (c) shows the map of Instrumental Intensity. Triangles correspond to the recording stations, red dots correspond the virtual stations obtained from the triangulation procedure while empty circle correspond to the phantom stations used to cover the area external to the seismic network. The labels F1, F2 and F3 identify the three fault segments which ruptured during the Irpinia earthquake.

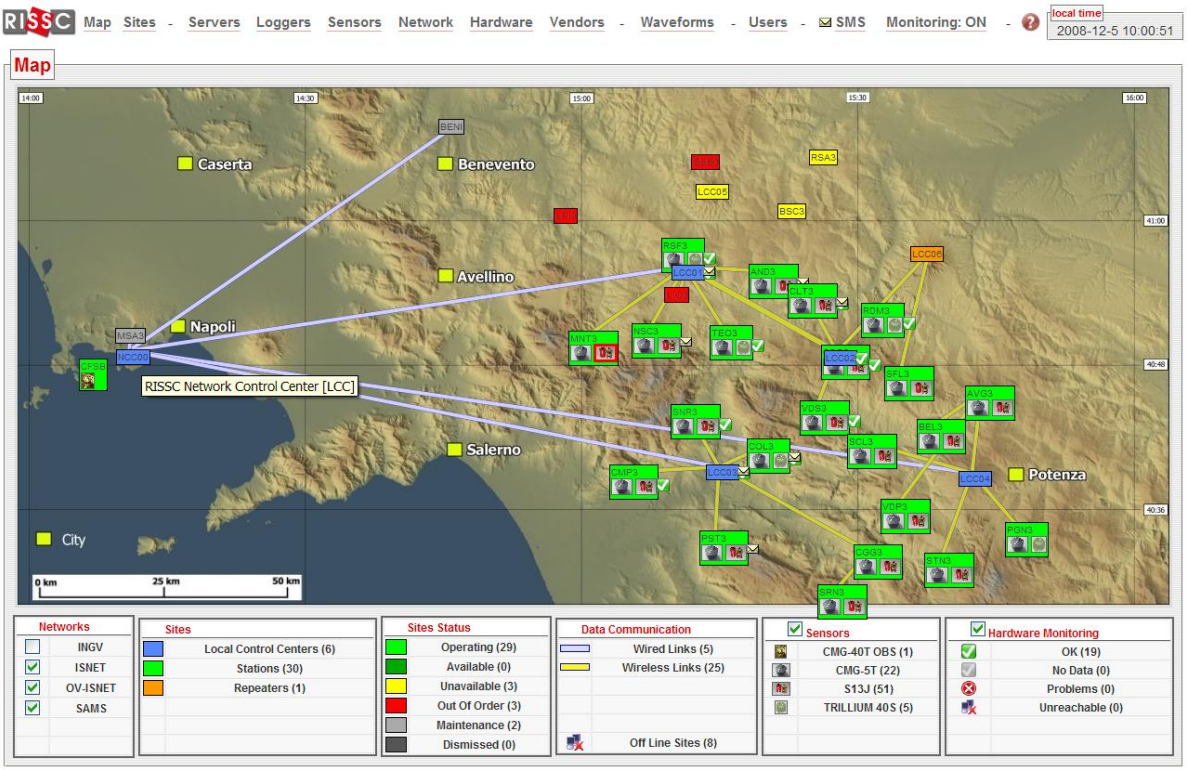

Figure 7: The map page of SeismNet Manager, showing the current overall state of ISNet. We can see: the Local Control Centers (in cyan), the stations (with a color coded working condition), the installed sensors (evidenced by a red outline if they have problems), the data links (high bandwidth ones are thicker), the alarms sent by the stations (mail icons), the internal state of the hardware (tick sign if all is well, blinking alert or no-connection icon otherwise).

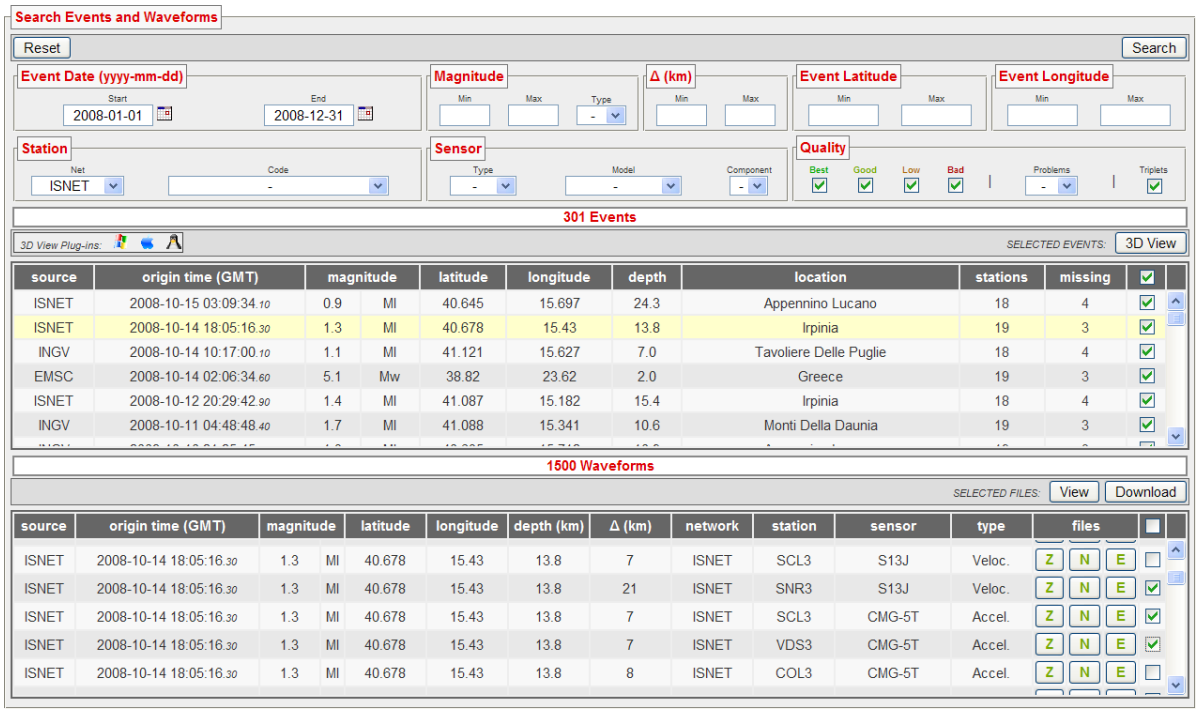

Figure 8: Events and waveforms can be searched using this interface. Events can be filtered for origin time, location, magnitude and distance to the stations. Waveforms can be filtered for seismic network, station, sensor and data quality.

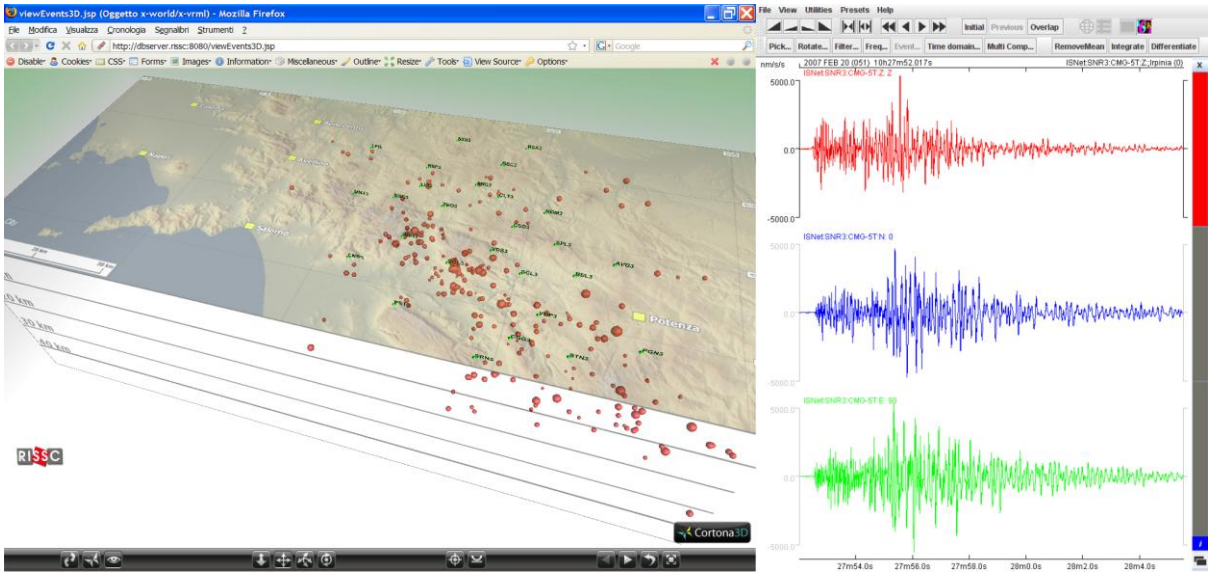

Figure 9: Events can displayed as an interactive 3D rendering in the web browser (left). Waveforms can be viewed and processed through the *SeisGram2K* Java applet (right). The parametric information associated to the waveforms (e.g. picks) can also be edited through this applet.